ELSEVIER

Journal of Organometallic Chemistry 568 (1998) 133–142

Journal of Organometallic Chemistry

# Phosphine derivatives of the 4-methylquinoline triosmium cluster $[(\mu\text{-H})Os_3(CO)_{10}\{\mu\text{-}1,2\text{-}\eta^2\text{-}C_9H_5(CH_3)N\}]$: crystal structures of two isomeric compounds $[(\mu\text{-H})Os_3(CO)_9\{\mu\text{-}1,2\text{-}\eta^2\text{-}C_9H_5(CH_3)N\}(PPh_3)]$ and $[(\mu\text{-H})Os_3(CO)_9\{\mu\text{-}1,2\text{-}\eta^2\text{-}C_9H_5(CH_3)N\}\{P(OMe)_3\}]$

Michael B. Hursthouse [a,*], Shariff E. Kabir [b], K.M. Abdul Malik [a], Markus Tesmer [b], Heinrich Vahrenkamp [b]

[a] *Department of Chemistry, University of Wales Cardiff, P.O. Box 912, Park Place, Cardiff CF1 3TB, Wales, UK*
[b] *Institut für Anorganische und Analytische Chemie, Universität Freiburg, Albertstr. 21, D-79104 Freiburg, Germany*

Received 13 February 1997

**Abstract**

The 4-methylquinoline triosmium cluster $[(\mu\text{-H})Os_3(CO)_{10}\{\mu\text{-}1,2\text{-}\eta^2\text{-}C_9H_5(CH_3)N\}]$ **9** reacts with $PPh_3$ at 110°C to give the mono and bis-substituted products $[(\mu\text{-H})Os_3(CO)_9\{\mu\text{-}1,2\text{-}\eta^2\text{-}C_9H_5(CH_3)N\}(PPh_3)]$ **10** and $[(\mu\text{-H})Os_3(CO)_8\{\mu\text{-}1,2\text{-}\eta^2\text{-}C_9H_5(CH_3)N\}(PPh_3)_2]$ **11,** respectively. Similarly the reaction of **9** with $P(OMe)_3$ gives $[(\mu\text{-H})Os_3(CO)_9\{\mu\text{-}1,2\text{-}\eta^2\text{-}C_9H_5(CH_3)N\}\{P(OMe)_3\}]$ **14** and $[(\mu\text{-H})Os_3(CO)_8\{\mu\text{-}1,2\text{-}\eta^2\text{-}C_9H_5(CH_3)N\}\{P(OMe)_3\}_2]$ **15**. Compound **10** exists as a mixture of three isomers in solution with the major (60%) having the $PPh_3$ ligand on the rear osmium atom and the hydride, which initially bridged the same edge as the 4-methylquinoline ligand, migrating to the carbon bound osmium and the phosphine bearing osmium edge. In contrast compound **14**, in which the $P(OMe)_3$ resides on the unbridged osmium atom and the hydride bridges the same edge as the 4-methylquinoline ligand, exists as two isomers in solution. The structures of **10** and **14** have been ascertained by X-ray crystal structure determination. Compound **11** exists as four isomers in solution and **15** as two isomers. 

*Keywords:* Osmium; 4-Methylquinoline; Crystal structure; Carbonyl; Phosphine

## 1. Introduction

The reactivity of trimetallic clusters containing nitrogen heterocycles with two-electron ligands such as phosphines, phosphites and isocyanides has recently been reported [1–5]. It has been demonstrated that the structures of the products obtained from such reactions are sensitive to the structure of the ligand and the steric bulk of the two electron donor ligands. For example, the reaction of $[(\mu\text{-H})Os_3(CO)_{10}(\mu\text{-}\eta^2\text{-}\overline{C{=}NCH_2CH_2CH_2})]$ **1** with triphenylphosphine at 98°C gives the substitution product $[(\mu\text{-H})Os_3(CO)_9(\mu\text{-}\eta^2\text{-}\overline{C{=}NCH_2CH_2CH_2})(PPh_3)]$ **2** (Scheme 1) in which the phosphine is at osmium atoms bridged by the hydride and the heterocyclic ligand [1].

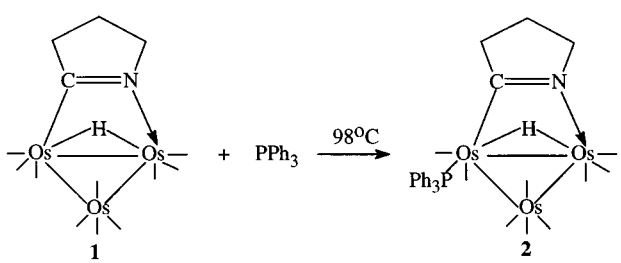


Scheme 1.

* Corresponding author. Fax: +44 1222 874029; e-mail: hursthouse@cardiff.ac.uk

0022-328X/98/$19.00 
*PII* S0022-328X(98)00762-1

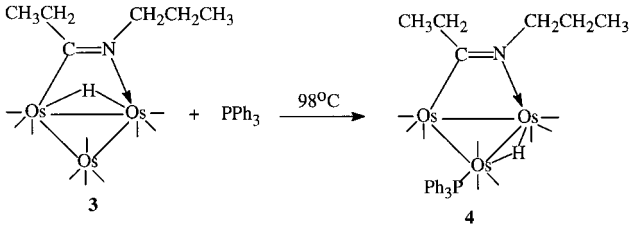


Scheme 2.

In contrast the acyclic compound [($\mu$-H)$Os_3(CO)_{10}$($\mu$-$\eta^2$-$CH_3CH_2C{=}NCH_2CH_2CH_3$)] **3** reacts with $PPh_3$ at 98°C to give the substitution product [($\mu$-H)$Os_3(CO)_9$($\mu$-$\eta^2$-$CH_3CH_2C{=}NCH_2CH_2CH_3$)-($PPh_3$)] **4** (Scheme 2) in which the hydride which initially bridged the same edge as the organic ligand has migrated [1].

It is interesting to note that no such rearrangement is observed when this compound is reacted with $P(OMe)_3$ and compound **5** (Scheme 3) analogous to **2** is obtained [1].

On the other hand, the 4-methylthiazolide cluster [($\mu$-H)$Os_3(CO)_{10}$($\mu$-2,3-$\eta^2$-C=NCMe=CHS)] **6** reacts with $PPh_3$ at 98°C to give mono and bis-substituted compounds [($\mu$-H)$Os_3(CO)_9$($\mu$-2,3-$\eta^2$-C=NCMe=CHS)($PPh_3$)] **7** and [($\mu$-H)$Os_3(CO)_8$($\mu$-2,3-$\eta^2$-C=NCMe=CHS)-($PPh_3$)$_2$] **8** (Scheme 4), respectively [5].

These studies have demonstrated that in addition to structural differences, the number of isomers observed in solution and the barriers to their interconversion are markedly dependent on the structure of the organic ligand and the steric bulk of the two electron donors. In our present work, we have investigated the reactions of [($\mu$-H)$Os_3(CO)_{10}$\{$\mu$-1,2-$\eta^2$-$C_9H_5(CH_3)N$\}] **9** with $PPh_3$ and $P(OMe)_3$. We have obtained distinctly different products from those reported previously [1–5] and structurally characterized two new isomeric compounds [($\mu$-H)$Os_3(CO)_9$\{$\mu$-1,2-$\eta^2$-$C_9H_5(CH_3)N$\}($PPh_3$)] **10** and [($\mu$-H)$Os_3(CO)_9$\{$\mu$-1,2-$C_9H_5(CH_3)N$\}\{$P(OMe)_3$\}] **14**. The results of this study are reported herein.

## 2. Results and discussion

The reaction of **9** with $PPh_3$ at 110°C leads to the isolation of the mono and bis-substituted products [($\mu$-H)$Os_3(CO)_9$\{$\mu$-1,2-$\eta^2$-$C_9H_5(CH_3)N$\}($PPh_3$)] **10** and [($\mu$-H)$Os_3(CO)_8$\{$\mu$-1,2-$\eta^2$-$C_9H_5(CH_3)N$\}($PPh_3$)$_2$] **11** in 30 and 42% yields, respectively. The infrared spectrum of **10** in the carbonyl stretching region is different from that of the related compounds **2** and **7**. The $^1$H-NMR spectrum of a recrystallized sample of **10** at −40°C shows three hydride signals, a doublet at $\delta$ −15.84 ($J_{P-H}$ = 14.7 Hz) and two singlets at $\delta$ −13.75 and −13.87 with a relative intensity of 3:1:1 (Fig. 1) as well as three singlets at $\delta$ 2.56, 2.41 and 2.45 for the methyl protons in similar integrated intensities indicating the presence of three isomers in solution.

The $^1$H-NMR data do not allow us to predict structures for these isomers and so an X-ray structure determination of the single crystals obtained from this isomeric mixture was undertaken. The solid state structure of the single crystals obtained from **10** revealed it to have structure **10a** (Scheme 5) with phosphine substituted on the unbridged osmium atom and the hydride bridging this osmium and the osmium atom sigma-bound to the carbon atom of the quinoline ligand. The X-ray structure of **10a** is shown in Fig. 2 and selected bond distances and angles are given in Table 1.

The structure contains a scalene triangle of osmium atoms with three distinctly different osmium–osmium bond lengths. There are three CO groups bonded to each osmium, in addition to a hydride and a 4-methylquinoline ligands bridging different edges of the triangle. The Os(2)–Os(3) bond [3.0442(10) Å] spanned by the hydride ligand is significantly longer than the other two Os–Os bonds [Os(1)–Os(2) = 2.7744(9) and Os(1)–Os(3) = 2.8731(9) Å]. This is consistent with the fact that a hydride bridging two metal atoms unaccompanied by other bridging groups causes a significant elongation of the metal-metal bond [6]. A similar lengthening of the hydride bridging Os–Os edge was observed in the related compound **14** [see later]. The quinoline bridged Os(1)–Os(2) edge [2.7744(9) Å] is significantly shorter than the unsupported Os(1)–Os(3) edge [2.8731(9) Å] which is similar to the average

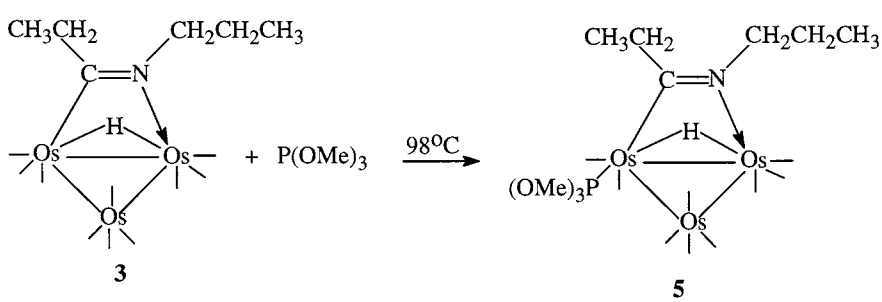


Scheme 3.

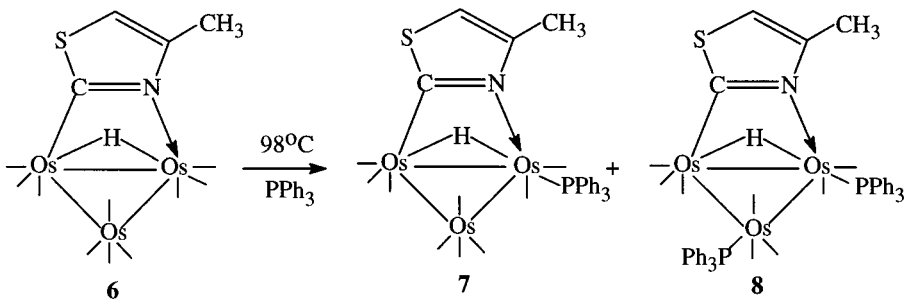


Scheme 4.

osmium–osmium bond length of 2.877(3) Å in $[Os_3(CO)_{12}]$ [7]. The triphenylphosphine is substituted at the rear osmium atom Os(3) and occupies an equatorial position. The metal-phosphine bond length, Os(3)–P(1) = 2.353(4) Å, is comparable with those of **2** [Os(2)–P = 2.371(2) Å] [1] and **7** [Os(3)–P = 2.376(3) Å] [5]. The 4-methylquinoline ligand bridges the Os(1)–Os(2) edge through the N(1) and C(10) atoms. The Os(2)–C(10) bond [2.068(13) Å] is significantly shorter and the Os(1)–N(1) bond [2.184(1) Å] is significantly longer than the corresponding values found in other related compounds [1–5]. In the methylquinoline ring, the N(1)–C(10) bond [1.32(2) Å] forming the bridge between Os(1) and Os(2) is significantly shorter than the N(1)–C(18) bond [1.41(2) Å] but quite close to the value quoted for C=N double bonds [1.25 Å] [8]; this indicates that the N=C double bond in the quinoline ligand has been lengthened only slightly by the bridge formation. This value is intermediate between those found in the $\mu$- and $\mu_3$-imidoyl clusters $[(\mu\text{-H})Os_3(CO)_9(\mu\text{-}\eta^2\text{-}CH_3CH_2C{=}NCH_2CH_2CH_3)(PPh_3)]$ (1.29 Å) and $[(\mu\text{-H})Os_3(CO)_8(\mu_3\text{-}\eta^2\text{-}CH_3CH_2C{=}NCH_2CH_2CH_3)(PPh_3)_2]$ (1.37 Å) [1]. The Os(1)–N(1)–C(10)–Os(2) bridge is nearly perpendicular to the triangle of the osmium atoms with a dihedral angle of 84.0(2)° between the two planes. The bridging hydride is found to lie very close to the plane of the $Os_3$ triangle. Other parameters related to the 4-methylquinoline, triphenyl phosphine and carbonyl ligands are as expected for these types of species.

By a combination of the variable temperature $^1$H-NMR data and the X-ray determined structure of **10** we can make structural assignment of the three observed isomers (Scheme 5). In the hydride region of the $^1$H-NMR spectrum the singlet resonances at $\delta$ −13.75 and −13.87 are due to the two minor radial isomers **10b** and **10c** while the doublet resonance at $\delta$ −15.84 can be assigned to the same structure as that found in the solid state structure **10a** with the phosphine on the rear osmium atom and the hydride ligand migrating to the carbon bound osmium and the phosphine bearing osmium edge. The magnitude of the phosphorus-hydrogen coupling constant of 14.7 Hz for the hydride doublet at $\delta$ −15.84 suggests that the hydride is trans to the phosphine and is consistent with those observed for related compounds in which the hydrides are trans to the phosphines and are coordinated to the same metal atoms [1,2,5], [9]a–c. As the temperature is increased to +25°C, the singlet resonances at $\delta$ −13.75 and

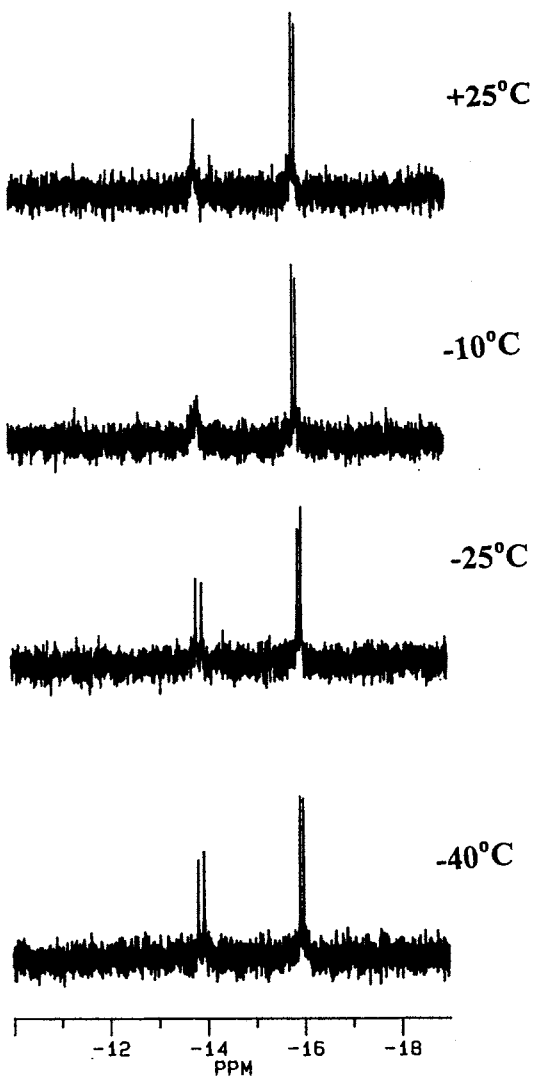


Fig. 1. Variable temperature $^1$H-NMR spectra of $[(\mu\text{-H})Os_3(CO)_9\{\mu\text{-}1,2\text{-}\eta^2\text{-}C_9H_5(CH_3)N\}(PPh_3)]$ **10** in the hydride region.

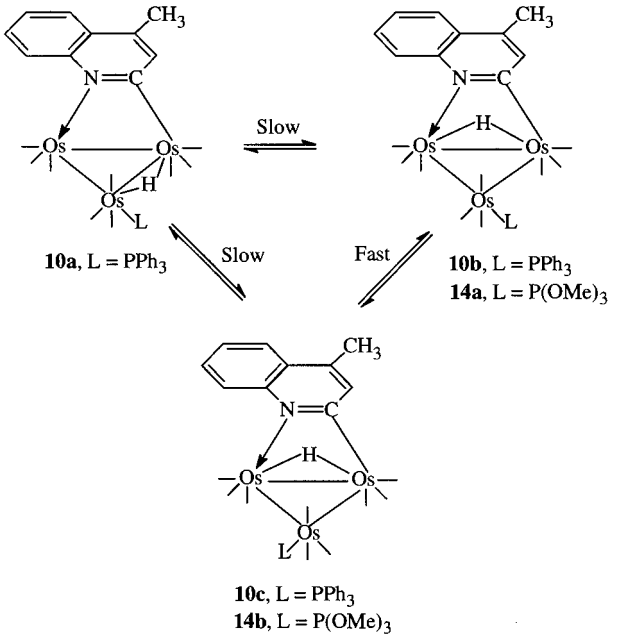


Scheme 5.

−13.87 average to a broadened singlet at δ −13.81 while the doublet at δ −15.84 remains unchanged. The equivalence of the hydride resonance at δ −13.75 and −13.87 can be explained by a fluxional process whereby two radial isomers interconvert by the usual trigonal twist mechanism which is rapid on the NMR time scale at room temperature. The structures and fluxional behavior of the two minor isomers are similar to those observed for the $PPh_3$ addition product of [($\mu$-H)$Os_3(CO)_9$($\mu_3$-$\eta^2$-C=$NCH_2CH_2CH_2$)] **12** which exists as two isomers in solution (Scheme 6, **13a** and **13b**). The structure of **13a** was confirmed earlier by a single crystal X-ray diffraction study [1].

It is of interest to note that in contrast to the two isomeric $PPh_3$ substituted derivatives **2** and **7** in which the $PPh_3$ ligand is at one of the two metal atoms bridged by the hydride and the heterocyclic ligand and which exist as two isomers in solution, cluster **10** exists as three isomers (Scheme 5) in solution with the $PPh_3$ substituted at the rear metal atom.

Although **10a** has a different structure from those of **2** and **7**, compound **11** is structurally similar to that of **8** [5]. The $^1$H-NMR spectrum of **11** at −40°C contains four doublets at δ −13.50 ($J_{P-H}$ = 13.5), −13.53 ($J_{P-H}$ = 13.4), −13.60 ($J_{P-H}$ = 14.4) and −13.80 ($J_{P-H}$ = 14.5 Hz) with relative intensities 1:3:1: 0.2 for hydrides as well as four resonances at δ 2.33, 2.28, 2.18 and 1.95 in similar relative integrated intensities for methyl protons indicating the presence of four isomers in solution. As the temperature is increased to +25°C the doublet resonances at δ −13.50 and −13.53 average to a doublet at δ −13.51 while the doublets at δ −13.60 and −13.80 average to a broadened singlet at δ −13.70. The variable temperature $^1$H-NMR spectra of **11** are very similar to those reported [5] for **8** and therefore they are expected to have similar structures and show similar coalescence behavior. But this could not be confirmed by an X-ray structure determination of **11**, since our repeated efforts to obtain suitable single crystals of this compound were unsuccessful. However, from the magnitude of phosphorus-hydrogen couplings observed for the hydride resonances of **11** at −40°C, their coalescence behavior compared with that of **8** [5] along with a knowledge of the solid state structure of the latter, we propose the four observed isomers of **11** to possess structures **11a–d** as shown in Scheme 7. We believe that the major isomer of **11** which exhibits the doublet hydride resonance at δ −13.53 has a structure similar to that reported for the major isomer of **8** having one phosphine ligand on the osmium atom bound to the nitrogen atom of the heterocyclic ring, the second phosphine on the rear osmium atom, and the hydride bridging the same edge as the heterocyclic ligand. The doublet at δ −13.50 which exchanges with the major doublet at δ −13.53 is due to the minor isomer **11b**. As reported for **8** [5], the hydride doublets at δ −13.60 and −13.80 which exchange to give a broadened singlet at δ −13.70 are due to the isomers **11c** and **11d** (Scheme 7) differing by the orientation of the phosphine bonded to the unbridged osmium atom. Further evidence for the above assignments comes from the fact that isomers **11a** and **11b** do not interconvert with **11c** and **11d** up to +50°C. The interconversion between isomers **11a** or **11b** and isomers **11c** or **11d** is slow because such an interconversion reaction would require phosphine dissociation which is a much higher energy process [1,2,5].

The reaction of **9** with $P(OMe)_3$ at 110°C in toluene also yields the mono- and bis-substituted products [($\mu$-H)$Os_3(CO)_9$\{$\mu$-1,2-$\eta^2$-$C_9H_5(CH_3)N$\}\{$P(OMe)_3$\}] **14** and [($\mu$-H)$Os_3(CO)_8$\{$\mu$-1,2-$\eta^2$-$C_9H_5(CH_3)N$\}\{$P(OMe)_3$\}$_2$] **15** in 40 and 46% yields, respectively. Both the compounds were characterized by infrared, $^1$H-NMR and elemental analysis together with X-ray diffraction study for **14.** The infrared spectrum of **14** is similar to that of **10** but their $^1$H-NMR spectra in the hydride region are different indicating that they have different structures. The $^1$H-NMR spectrum of **14** at 25°C exhibits a slightly broadened singlet hydride resonance at δ −14.12 which is resolved into two sharp singlets at δ −14.11 and −14.14 with relative intensities 2:1 at −40°C. Two doublets at δ 3.66 and 3.56 in a 2:1 relative ratio are observed which can be attributed to the methyl protons of the $P(OMe)_3$ ligand. Two singlets at δ 2.44 and 2.46 in a 2:1 ratio due to the methyl protons of 4-methyl quinoline are also observed. The $^{31}$P\{$^1$H\}-NMR spectrum of **14** contains two singlets at δ 104.1 and 103.2 with a relative intensity of 2:1. From the above spectroscopic data, we suggest that **14** exists as two radial isomers (**14a** and **14b**) in solution with the trimethyl

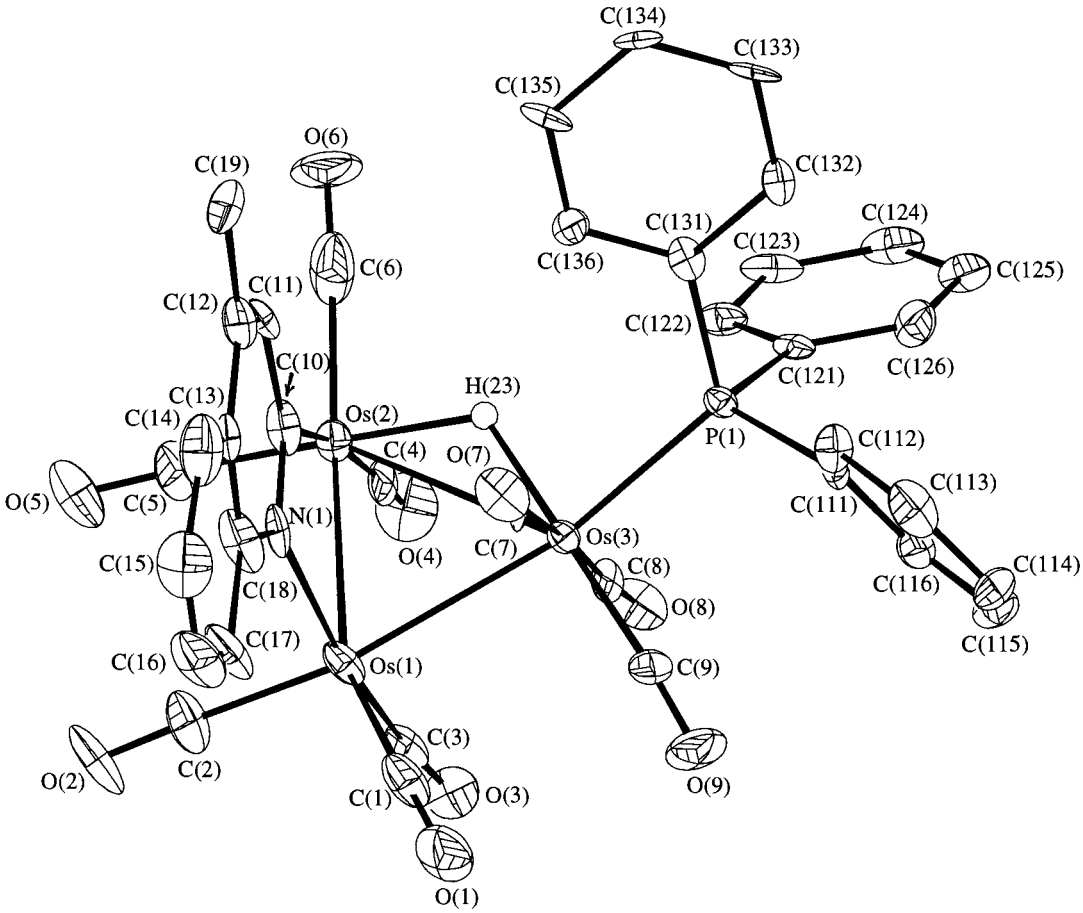


Fig. 2. Solid state structure of $[(\mu\text{-H})Os_3(CO)_9\{\mu\text{-1,2-}\eta^2\text{-}C_9H_5(CH_3)N\}(PPh_3)]$ **10** showing the atom labelling scheme. Thermal ellipsoids are drawn at 50% probability level. The ring hydrogen atoms are omitted for clarity.

phosphite substituted at the rear metal atom. As mentioned above for the two minor isomers of **10**, these two isomers interconvert by the usual trigonal twist mechanism on the NMR time scale at room temperature.

The identity of the compound **14** was unambiguously determined by a single crystal study. The molecular structure of this compound is shown in Fig. 3 and selected bond distances and angles are given in Table 2.

The structure consists of an osmium triangle with three metal-metal bonds: Os(1)–Os(3) = 2.8653(6), Os(2)–Os(3) = 2.8799(7) and Os(1)–Os(2) = 2.9282(6) Å, one of which is considerably longer than the other two. As indicated by the spectroscopic data, the trimethyl phosphite ligand is substituted at the rear osmium atom Os(3) and occupies an equatorial site. Os(3) is also coordinated to three terminal carbonyls, one in an equatorial site and two in axial sites. The metal-phosphorus bond length, Os(3)–P(1) = 2.279(3) Å is somewhat shorter than that in **10**, but comparable with those observed for other phosphite complexes, e.g. $[Os_3(CO)_{10}\{P(OMe)_3\}_2]$ ($Os–P_{av}$ = 2.286 Å) [10] and $[(\mu\text{-H})Os_6(CO)_{20}\{P(OMe)_3\}_2(\mu\text{-}PH_2)]$ [$Os–P_{av}$ = 2.276(9) Å] [11]. The 4-methylquinoline ligand bridges the longest Os(1)–Os(2) edge through the N(1) and C(13) atoms of the heterocyclic moiety. The Os(1)–Os(2) edge of the cluster is also bridged by a hydride ligand on the opposite side with respect to the organic ligand. The bridged Os(1)–Os(2) distance is longer than the two unbridged Os–Os edges (by ca. 0.015 Å) but the average value of 2.8726(6) Å is not significantly different from the average value for the Os–Os bond [2.877(3) Å] in $[Os_3(CO)_{12}]$ [7]. The presence of the bridging hydride results in an opening of the Os(1)–Os(2)–C(7) and Os(2)–Os(1)–C(1) angles [115.3(3) and 115.0(3)°, respectively]. The Os(1)–C(13)–N(1)–Os(2) bridge is nearly perpendicular to the triangle of the osmium atoms with a dihedral angle of 76.4(2)° between the two planes. The hydride ligand which bridges the same Os–Os edge as the quinoline ligand does not lie in the $Os_3$ plane as observed in **10**; instead it makes a dihedral angle of 58° with the latter. The Os–N–C–Os bridge in none of the compounds **10** or **14** is exactly planar, but somewhat twisted, as shown by the relevant Os–N–C–Os torsion angles 5.6(1.1) in **10** and 5.4(9)° in **14**. These deviations from planarity with slight twists may be attributed to

Table 1
Selected bond lengths (Å) and angles (°) for [($\mu$-H)$Os_3(CO)_9$\{$\mu$-1,2-$\eta^2$-$C_9H_5(CH_3)N$\}($PPh_3$)] 10

| | | | |
|---|---|---|---|
| Os(1)–Os(2) | 2.7744(9) | Os(1)–Os(3) | 2.8731(9) |
| Os(2)–Os(3) | 3.0442(10) | Os(1)–C(3) | 1.88(2) |
| Os(1)–C(2) | 1.90(2) | Os(1)–C(1) | 1.91(2) |
| Os(1)–N(1) | 2.184(11) | Os(2)–C(5) | 1.86(2) |
| Os(2)–C(4) | 1.95(2) | Os(2)–C(6) | 1.95(2) |
| Os(2)–C(10) | 2.068(13) | Os(3)–C(9) | 1.88(2) |
| Os(3)–C(7) | 1.929(13) | Os(3)–C(8) | 1.95(2) |
| Os(3)–P(1) | 2.353(4) | Os(2)–H(23) | 1.75[a] |
| Os(3)–H(23) | 1.84[a] | | |
| C(3)–Os(1)–C(2) | 92.8(7) | C(3)–Os(1)–C(1) | 90.7(6) |
| C(2)–Os(1)–C(1) | 101.4(7) | C(3)–Os(1)–N(1) | 166.6(5) |
| C(2)–Os(1)–N(1) | 91.6(6) | C(1)–Os(1)–N(1) | 100.8(6) |
| C(3)–Os(1)–Os(2) | 97.3(4) | C(2)–Os(1)–Os(2) | 102.2(5) |
| C(1)–Os(1)–Os(2) | 154.6(5) | N(1)–Os(1)–Os(2) | 69.4(3) |
| C(3)–Os(1)–Os(3) | 85.2(5) | C(2)–Os(1)–Os(3) | 166.8(5) |
| C(1)–Os(1)–Os(3) | 91.7(5) | N(1)–Os(1)–Os(3) | 87.6(3) |
| Os(2)–Os(1)–Os(3) | 65.21(3) | C(5)–Os(2)–C(4) | 91.1(6) |
| C(5)–Os(2)–C(6) | 97.9(7) | C(4)–Os(2)–C(6) | 96.2(7) |
| C(5)–Os(2)–C(10) | 88.1(6) | C(4)–Os(2)–C(10) | 170.2(6) |
| C(6)–Os(2)–C(10) | 93.6(7) | C(5)–Os(2)–Os(1) | 88.3(5) |
| C(4)–Os(2)–Os(1) | 99.9(4) | C(6)–Os(2)–Os(1) | 162.7(6) |
| C(10)–Os(2)–Os(1) | 70.4(4) | C(5)–Os(2)–Os(3) | 147.1(5) |
| C(4)–Os(2)–Os(3) | 91.8(4) | C(6)–Os(2)–Os(3) | 114.3(5) |
| C(10)–Os(2)–Os(3) | 83.7(4) | Os(1)–Os(2)–Os(3) | 58.96(2) |
| C(9)–Os(3)–C(7) | 86.3(6) | C(9)–Os(3)–C(8) | 89.6(6) |
| C(7)–Os(3)–C(8) | 174.7(6) | C(9)–Os(3)–P(1) | 94.2(5) |
| C(7)–Os(3)–P(1) | 89.9(4) | C(8)–Os(3)–P(1) | 93.8(5) |
| C(9)–Os(3)–Os(1) | 93.5(5) | C(7)–Os(3)–Os(1) | 81.3(4) |
| C(8)–Os(3)–Os(1) | 95.6(4) | P(1)–Os(3)–Os(1) | 167.90(8) |
| C(9)–Os(3)–Os(2) | 148.6(5) | C(7)–Os(3)–Os(2) | 94.8(4) |
| C(8)–Os(3)–Os(2) | 86.9(4) | P(1)–Os(3)–Os(2) | 117.25(8) |
| Os(1)–Os(3)–Os(2) | 55.83(2) | Os(2)–H(23)–Os(3) | 116[a] |

[a] The parameters involving the bridging hydride H(23) are only approximate and should be treated with caution.

the tendency to relieve strain associated with the bridge formation. The two N–C bonds in the methylquinoline ring show the same trend as observed in **10**, i.e. the bridging N–C bond [1.309(12) Å] is significantly shorter than the other N–C bond [1.438(12) Å], the former retaining most of its double bond character. In **14**, the Os–N and Os–C(bridge) bonds [2.141(9) and 2.101(10) Å], respectively, are slightly shorter and longer than the corresponding values [2.184(11) and 2.068(13) Å] in **10**. The remaining molecular dimensions are as expected.

It may be noted here that not only do the minor

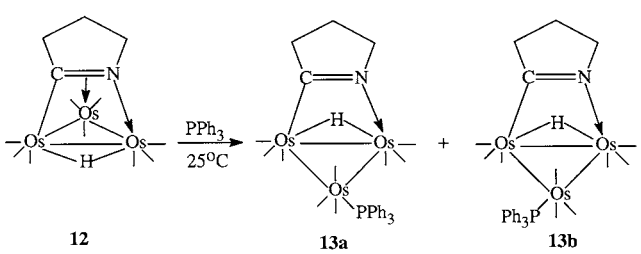


Scheme 6.

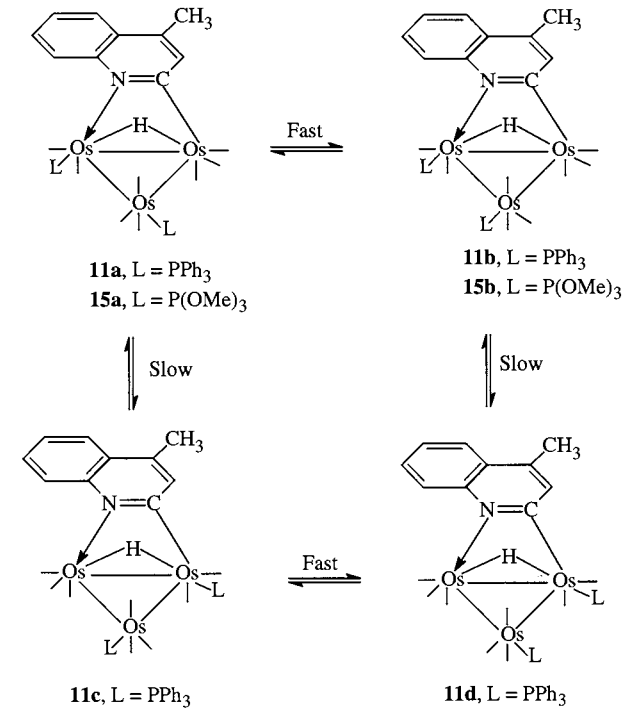


Scheme 7.

isomers of **10** become the major isomers in the case of **14**, the major isomer of **10** does not have its counterpart in detectable amount in the case of **14**, illustrating

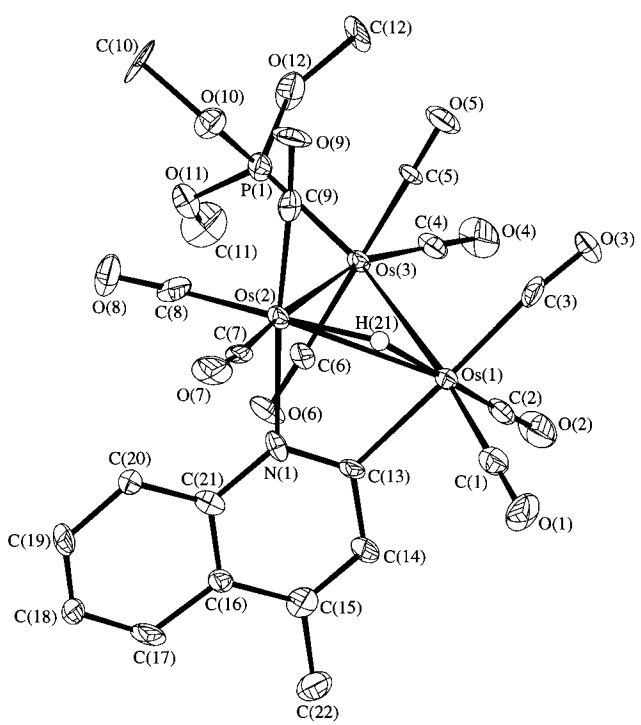


Fig. 3. Solid state structure of [($\mu$-H)$Os_3(CO)_9$\{$\mu$-1,2-$\eta^2$-$C_9H_5(CH_3)N$\}\{$P(OMe)_3$\}] **14** showing the atom labelling scheme. Thermal ellipsoids are drawn at 50% probability level. The ring hydrogen atoms are omitted for clarity.

Table 2
Selected bond lengths (Å) and angles (°) for [($\mu$-H)$Os_3(CO)_9$\{$\mu$-1,2-$\eta^2$-$C_9H_5(CH_3)N$\}\{$P(OMe)_3$\}] 14

| | | | |
|---|---|---|---|
| Os(1)–Os(3) | 2.8653(6) | Os(1)–Os(2) | 2.9282(6) |
| Os(2)–Os(3) | 2.8799(7) | Os(1)–C(2) | 1.864(12) |
| Os(1)–C(1) | 1.902(12) | Os(1)–C(3) | 1.976(12) |
| Os(1)–C(13) | 2.101(10) | Os(2)–C(8) | 1.880(12) |
| Os(2)–C(7) | 1.887(13) | Os(2)–C(9) | 1.887(13) |
| Os(2)–N(1) | 2.141(9) | Os(3)–C(5) | 1.896(11) |
| Os(3)–C(4) | 1.902(13) | Os(3)–C(6) | 1.922(12) |
| Os(3)–P(1) | 2.279(3) | Os(1)–H(21) | 1.64[a] |
| Os(2)–H(21) | 1.68[a] | | |
| C(2)–Os(1)–C(1) | 99.2(5) | C(2)–Os(1)–C(3) | 92.2(4) |
| C(1)–Os(1)–C(3) | 94.1(4) | C(2)–Os(1)–C(13) | 89.6(4) |
| C(1)–Os(1)–C(13) | 86.7(4) | C(3)–Os(1)–C(13) | 178.0(4) |
| C(2)–Os(1)–Os(3) | 84.4(3) | C(1)–Os(1)–Os(3) | 174.0(3) |
| C(3)–Os(1)–Os(3) | 90.5(3) | C(13)–Os(1)–Os(3) | 88.6(3) |
| C(2)–Os(1)–Os(2) | 136.3(3) | C(1)–Os(1)–Os(2) | 115.0(3) |
| C(3)–Os(1)–Os(2) | 110.7(3) | C(13)–Os(1)–Os(2) | 67.3(3) |
| Os(3)–Os(1)–Os(2) | 59.60(2) | C(8)–Os(2)–C(7) | 98.4(5) |
| C(8)–Os(2)–C(9) | 90.3(4) | C(7)–Os(2)–C(9) | 90.6(5) |
| C(8)–Os(2)–N(1) | 93.7(4) | C(7)–Os(2)–N(1) | 90.8(4) |
| C(9)–Os(2)–N(1) | 175.5(4) | C(8)–Os(2)–Os(3) | 88.3(3) |
| C(7)–Os(2)–Os(3) | 173.0(3) | C(9)–Os(2)–Os(3) | 87.6(4) |
| N(1)–Os(2)–Os(3) | 90.5(2) | C(8)–Os(2)–Os(1) | 140.9(3) |
| C(7)–Os(2)–Os(1) | 115.3(3) | C(9)–Os(2)–Os(1) | 107.8(3) |
| N(1)–Os(2)–Os(1) | 67.7(2) | Os(3)–Os(2)–Os(1) | 59.113(14) |
| C(5)–Os(3)–C(4) | 93.4(5) | C(5)–Os(3)–C(6) | 172.5(5) |
| C(4)–Os(3)–C(6) | 93.0(5) | C(5)–Os(3)–P(1) | 90.6(3) |
| C(4)–Os(3)–P(1) | 95.5(3) | C(6)–Os(3)–P(1) | 92.6(3) |
| C(5)–Os(3)–Os(1) | 86.2(3) | C(4)–Os(3)–Os(1) | 103.5(3) |
| C(6)–Os(3)–Os(1) | 88.5(3) | P(1)–Os(3)–Os(1) | 160.83(8) |
| C(5)–Os(3)–Os(2) | 88.0(3) | C(4)–Os(3)–Os(2) | 164.6(3) |
| C(6)–Os(3)–Os(2) | 84.8(3) | P(1)–Os(3)–Os(2) | 99.75(8) |
| Os(1)–Os(3)–Os(2) | 61.29(2) | Os(1)–H(21)–Os(2) | 124[a] |

[a] The parameters involving the bridging hydride H(21) are only approximate and should be treated with caution.

the sensitivity of isomer distribution to the steric bulk of the phosphine ligand.

We were unable to obtain X-ray quality crystals of **15**; therefore, its structural assignment is based on spectroscopic data and elemental analysis. The $^1$H-NMR spectrum of **15** at −40°C (Fig. 4) shows two doublets of doublets in an approximate 1:1 ratio at $\delta$ −14.38 ($J$ = 11.5, 2.2 Hz) and −14.29 ($J$ = 11.4, 1.8 Hz) indicating the presence of two isomers in solution which is in sharp contrast to **11**. As the temperature is increased the hydride resonances are broadened and averaged to a doublet at $\delta$ −14.33 ($J$ = 11.5 Hz) at 25°C. The hydride signals appear as doublets of doublets because of three-bond phosphorus–hydride couplings. There are numerous examples in the literature for the observation of small (1–3 Hz) phosphorus–hydride three bond couplings in metal clusters [1,12]a, [12]b–c. Based on the crystal structure of **8** and the solution dynamics of **8** and **11**, we can assign these two isomeric bis-phosphite substituted products to structures **15a** and **15b**.

The significance of this work is the demonstration that changes in the structure of the heterocyclic ligands as well as the steric bulk of the phosphine ligands have important impact on the structures of the substituted products and their isomers distribution.

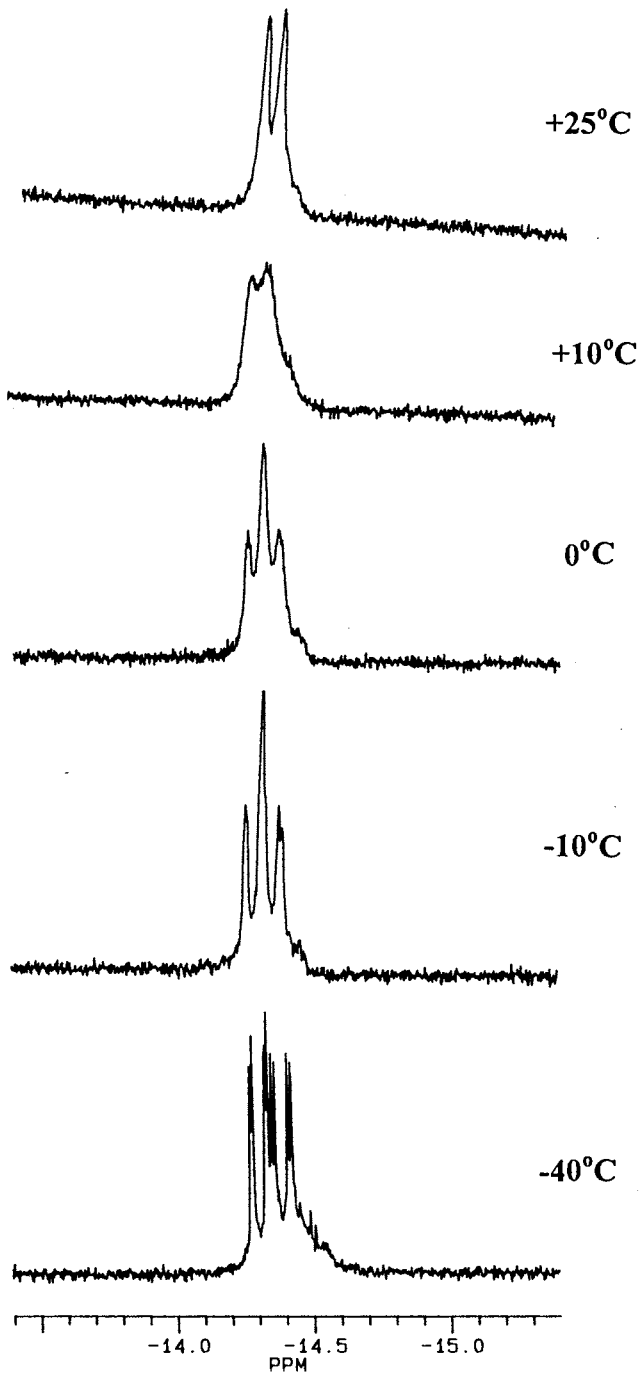


Fig. 4. Variable temperature $^1$H-NMR spectra of [($\mu$-H)$Os_3(CO)_8$\{$\mu$-1,2-$\eta^2$-$C_9H_5(CH_3)N$\}\{$P(OMe)_3$\}$_2$] **15** in the hydride region.

## 3. Experimental

Although the reaction products are air stable, all the reactions were performed under an atmosphere of prepurified nitrogen. The solvents were distilled according to the standard procedure immediately before use. IR spectra were recorded on a Perkin-Elmer 1420 spectrophotometer. $^1$H-and $^{31}$P{$^1$H}-NMR spectra were recorded on Bruker AC 200 spectrometer. Chemical shifts for the $^{31}$P{$^1$H}-spectra are relative to 85% $H_3PO_4$. Elemental analyses were performed in the microanalytical laboratory, Institut für Anorganische und Analytische Chemie, Universität Freiburg. The starting cluster **9** was prepared according to the published procedure ([13]a,b). Triphenylphosphine and trimethyl phosphite were purchased from Aldrich and used as received.

### 3.1. Reaction of 9 with $PPh_3$

To a toluene solution (30 ml) of compound **9** (0.105 g, 0.106 mmol) in a flame-dried Schlenk flask was added $PPh_3$ (0.059 g, 0.225 mmol) and the reaction mixture was heated to reflux for 8 h. The solvent was removed in vacuo and the residue was chromatographed by TLC plates eluting with hexane/$CH_2Cl_2$ (10:3, v/v) to give three bands. The faster moving band gave unreacted **9** (0.008 g). The second band gave [($\mu$-H)$Os_3$(CO)$_9${$\mu$-1,2-$\eta^2$-$C_9H_5(CH_3)$N}-($PPh_3$)] **10** (0.039 g, 30%) as yellow crystals after recrystallization from hexane/$CH_2Cl_2$ at −20°C. (Anal. Found: C, 36.32; H, 1.99; N, 1.13. $C_{37}H_{24}NO_9Os_3P$. Calc.: C, 36.18; H, 1.97; N, 1.14%). IR($\nu$CO, $CH_2Cl_2$): 2081sh, 2077m, 2047vs, 2018vs, 1998vs, 1974m, 1957m, 1938m cm$^{-1}$. $^1$H-NMR ($CD_2Cl_2$, −40°C): mixture of three isomers, $\delta$ 7.77–6.39 (m, 20 H), 2.56 (s, 3H), 2.41 (s, 3H), 2.45 (s, 3H), −13.75 (s, 1H), −13.87 (s, 1H), −15.84 (d, 1H, $J_{P-H}$ = 14.7 Hz). The phenyl protons resonances of $PPh_3$ and the ring protons resonances of 4-methylquinoline of **10** are overlapped. The third band afforded [($\mu$-H)$Os_3$(CO)$_8${$\mu$-1,2-$\eta^2$-$C_9H_5(CH_3)$N}($PPh_3$)$_2$] **11** (0.065 g, 42%) as orange crystals after recrystallization from hexane/$CH_2Cl_2$ at −20°C. (Anal. Found: C, 43.88; H, 2.79; N, 1.00. $C_{54}H_{39}NO_8Os_3P_2$. Calc.: C, 44.35; H, 2.69; N, 0.96%). IR($\nu$CO, $CH_2Cl_2$): 2058m, 2017vs, 1988s, 1976s, 1947s cm$^{-1}$; $^1$H-NMR ($CD_2Cl_2$, −40°C): $\delta$ 7.09–7.55 (m, 35H), 2.33 (s, 3H), 2.28 (s, 3H), 2.18 (s, 3H), 1.95 (s, 3H), -13.50 (d, 1H, $J_{P-H}$ = 13.5 Hz), −13.53 (d, 1H, $J_{P-H}$ = 13.4 Hz), −13.60 (d, 1H, $J_{P-H}$ = 14.4 Hz), −13.80 (d, 1H, $J_{P-H}$ = 14.5 Hz). The signals due to the phenyl protons of the $PPh_3$ ligands and the ring protons of the 4-methylquinoline for these isomers are overlapped.

### 3.2. Reaction of 9 with $P(OMe)_3$

$P(OMe)_3$ (27 μl, 0.226 mmol) was added to a toluene solution (25 ml) of **9** (0.075 g, 0.075 mmol). The resulting solution was heated to reflux for 7 h. All the volatiles were removed in vacuo. Chromatographic separation of the residue by TLC on silica gel eluting with hexane/$CH_2Cl_2$ (5:1, v/v) resolved three bands. The faster moving band afforded unreacted **9** (0.005 g) while the second band gave [($\mu$-H)$Os_3$(CO)$_9${$\mu$-1,2-$\eta^2$-$C_9H_5(CH_3)$N}{P(OMe)$_3$}] **14** (0.033 g, 40%) as yellow crystals after recrystallization from hexane/$CH_2Cl_2$ at −20°C. (Anal. Found: C, 24.52; H, 1.85; N, 1.35. $C_{22}H_{18}NO_{12}Os_3P$. Calc.: C, 24.24; H, 1.66; N, 1.29%). IR($\nu$CO, $CH_2Cl_2$): 2080m, 2049vs, 2023s, 1997vs, 1975s, 1960sh cm$^{-1}$. $^1$H-NMR ($CD_2Cl_2$, −40°C): mixture of two isomers, major isomer, $\delta$ 7.81 (m, 3H), 7.41 (m, 2H), 3.66 (d, 9H, $J_{P-H}$ = 12.1 Hz), 2.44 (s, 3H), −14.11 (s, 1H); minor isomer, $\delta$ 7.81 (m, 3H), 7.41 (m, 2H), 3.56 (d, 9H, $J_{P-H}$ = 12.4 Hz), 2.34 (s, 3H), −14.14 (s, 1H). $^{31}$P{$^1$H}-NMR($CD_2Cl_2$): major isomer, $\delta$ 104.1 (s), minor isomer, 103.2 (s). The third band yielded [($\mu$-H)$Os_3$(CO)$_8${$\mu$-1,2-$\eta^2$-$C_9H_5(CH_3)$N}{P(OMe)$_3$}$_2$] **15** (0.041 g, 46%) as orange crystals after recrystallization from hexane/$CH_2Cl_2$ at −20°C. Anal. Found: C, 24.45; H, 2.34; N, 1.20. $C_{24}H_{27}NO_{14}Os_3P_2$. Calc.: C, 24.30; H, 2.29; N, 1.18%). IR ($\nu$CO, $CH_2Cl_2$): 2062s, 2025vs, 1996s, 1983vs, 1965sh, 1957s, 1939w cm$^{-1}$; $^1$H-NMR ($CD_2Cl_2$): mixture of two isomers; $\delta$ 7.74(m, 3H), 7.37(m, 1H), 7.25 (m, 1H), 3.51 (d, 9H, $J_{P-H}$ = 11.6 Hz), 3.42 (d, 9H, $J_{P-H}$ = 11.5 Hz), 2.42 (s, 3H), 2.40 (s, 3H), −14.38 (dd, 1H, $J_{P-H}$ = 11.5, 2.2 Hz), −14.29(dd, 1H, $J_{P-H}$ = 11.4, 1.8 Hz).

### 3.3. X-ray crystallography

Crystals of the complexes **10** and **14** were obtained as described above. All measurements were made using a Delft Instruments FAST TV area detector diffractometer positioned at the window of a rotating anode (Mo) generator, in a manner described previously [14]. In both cases the unit cell parameters were obtained by least-squares refinement of the diffractometer angles for 250 reflections. The crystallographic data, and the data collection and refinement details for the compounds are presented in Table 3.

Both data sets were corrected for absorption using DIFABS [15]. The structures were solved by direct methods (SHELXS-86) [16], developed via difference syntheses, and refined on $F^2$ by full-matrix least-squares (SHELXL-93) [17] using all unique data with intensities greater than 0. In both cases the non-hydrogen atoms were anisotropic, and the hydrogen atoms belonging to the quinoline and phenyl rings included in calculated

Table 3
Crystal data and details of data collection and structure refinement for $[(\mu\text{-H})Os_3(CO)_9\{\mu\text{-1,2-}\eta^2\text{-}C_9H_5(CH_3)N\}(L)]$ (L = $PPh_3$ **10** or $P(OMe)_3$ **14**)[a]

| | **10** | **14** |
|---|---|---|
| Empirical formula | $C_{37}H_{24}NO_9Os_3P$ | $C_{22}H_{18}NO_{12}Os_3P$ |
| Formula weight | 1228.14 | 1089.94 |
| Crystal system | Triclinic | Monoclinic |
| Space group | $P\bar{1}$ (no. 2) | $P2_1/c$ (no. 14) |
| $a$ (Å) | 9.977(2) | 14.158(2) |
| $b$ (Å) | 13.359(2) | 16.649(2) |
| $c$ (Å) | 13.432(2) | 11.994(2) |
| $\alpha$ (°) | 81.66(2) | 90 |
| $\beta$ (°) | 85.41(2) | 105.219(8) |
| $\gamma$ (°) | 82.091(11) | 90 |
| $V$ (Å$^3$) | 1751.3(5) | 2728.2(7) |
| $Z$ | 2 | 4 |
| $D_{calc.}$ (Mg m$^{-3}$) | 2.329 | 2.654 |
| Absorption coefficient (mm$^{-1}$) | 10.959 | 14.058 |
| $F(000)$ | 1136 | 1984 |
| Crystal size (mm) | $0.32\times0.22\times0.07$ | $0.12\times0.08\times0.06$ |
| Theta range for data collection (°) | 2.03–24.86 | 1.93–24.99 |
| $h_{min}$, $h_{mmax}$; $k_{min}$, $k_{max}$; $l_{min}$, $l_{max}$ | −11, 10; −15, 15; −15, 11 | −15, 9; −19, 19; −11, 12 |
| Reflections collected | 7351 | 8890 |
| Independent reflections | 4822 | 3982 |
| $R_{int}$ | 0.0955 | 0.0772 |
| Absorption correction factors | 0.723–0.998 | 0.789–1.191 |
| Data/restraints/parameters | 4822/36/425 | 3982/18/356 |
| Goodness-of-fit on $F^2$ | 1.066 | 0.859 |
| $R_1/wR_2$ (all unique data) | 0.0647/0.1418 | 0.0455/0.0661 |
| $R_1/wR_2$ [data with $I>2\sigma(I)$] | 0.0581/0.1397 | 0.0312/0.0642 |
| Largest diff. peak and hole (e Å$^{-3}$) | 2.111 and −2.340 | 2.117 and −1.253 |

[a] Details in common: Mo–$K_\alpha$ radiation, $\lambda = 0.71069$ Å, $T = 150(2)$ K, cell dimensions from 250 reflections, full-matrix least-squares on $F^2$; $R_1$ and $wR_2$ as defined in [17]; weighting scheme, $w = 1/[\sigma^2(F_o^2) + (a*P)^2]$, where $P = [\max(F_o^2) + 2F_c^2)]/3$ and $a = 0.0861$ for **10** and 0.0109 for **14**.

positions (riding model). The bridging hydrides [H(23) in **10** and H(21) in **14**] were located from difference maps but not refined. Several atoms [C(2), C(5) and C(15) in **10**, and C(3), O(2), O(4), O(5), O(6) and O(8) in **14**] were refined with the restraints ISOR = 0.005 and 0.01, respectively, to keep the displacement coefficients of these atoms 'approximately isotropic'. Final $R$-values are given in Table 3. Sources of scattering factors are as in [17]. The molecular diagrams were drawn using SNOOPI [18]. Fractional atomic co-ordinates are given in Tables 4 and 5.

Full crystallographic details including thermal parameters and bond lengths and angles have been deposited at the Cambridge Crystallographic Data Centre (CCDC). Any request to the CCDC for this material should quote the full literature citation.

Table 4
Atomic coordinates ($\times10^4$) and equivalent isotropic displacement parameters (Å$^2\times10^3$) for $[(\mu\text{-H})Os_3(CO)_9\{\mu\text{-1,2-}\eta^2\text{-}C_9H_5(CH_3)N\}(PPh_3)]$ **10**

| | $x$ | $y$ | $z$ | $U_{eq}$[a] |
|---|---|---|---|---|
| Os(1) | 3880.0(6) | 2306.7(4) | 4105.6(4) | 22(1) |
| Os(2) | 1498.5(6) | 1514.8(4) | 3915.2(4) | 21(1) |
| Os(3) | 3389.1(6) | 2060.1(4) | 2081.9(4) | 15(1) |
| P(1) | 2563(3) | 2088(2) | 485(3) | 14(1) |
| O(1) | 6244(12) | 3510(9) | 3368(9) | 45(3) |
| O(2) | 3960(14) | 2202(9) | 6368(9) | 49(3) |
| O(3) | 5761(10) | 340(8) | 4015(8) | 35(3) |
| O(4) | 2582(12) | −785(8) | 4068(10) | 45(3) |
| O(5) | 1083(13) | 1337(10) | 6182(9) | 53(3) |
| O(6) | −1409(12) | 1301(10) | 3449(10) | 50(3) |
| O(7) | 2604(11) | 4381(7) | 1884(8) | 32(3) |
| O(8) | 4498(11) | −228(8) | 2220(9) | 33(3) |
| O(9) | 6149(10) | 2634(9) | 1294(10) | 42(3) |
| N(1) | 2157(12) | 3510(8) | 4043(8) | 20(3) |
| C(1) | 5336(18) | 3084(11) | 3641(12) | 30(4) |
| C(2) | 3909(17) | 2255(11) | 5526(12) | 32(4) |
| C(3) | 5065(15) | 1081(11) | 4092(11) | 25(3) |
| C(4) | 2193(15) | 72(13) | 3985(11) | 27(4) |
| C(5) | 1210(17) | 1390(12) | 5310(13) | 34(4) |
| C(6) | −336(22) | 1380(14) | 3596(14) | 48(5) |
| C(7) | 2851(13) | 3511(10) | 2005(10) | 17(3) |
| C(8) | 4091(14) | 617(12) | 2202(11) | 25(4) |
| C(9) | 5106(15) | 2386(12) | 1560(12) | 28(4) |
| C(10) | 1096(15) | 3079(10) | 3885(11) | 22(3) |
| C(11) | −162(14) | 3741(10) | 3651(10) | 19(3) |
| C(12) | −257(15) | 4781(11) | 3573(11) | 27(4) |
| C(13) | 898(14) | 5216(10) | 3795(11) | 21(3) |
| C(14) | 887(19) | 6282(12) | 3759(13) | 41(5) |
| C(15) | 2029(19) | 6667(13) | 4042(14) | 42(5) |
| C(16) | 3122(19) | 6045(13) | 4301(13) | 37(4) |
| C(17) | 3204(19) | 4963(13) | 4321(12) | 38(4) |
| C(18) | 2080(18) | 4564(10) | 4084(12) | 30(4) |
| C(19) | −1576(15) | 5448(13) | 3260(13) | 38(4) |
| C(111) | 3687(8) | 2695(6) | −476(6) | 19(3) |
| C(112) | 3424(7) | 3738(5) | −784(7) | 21(3) |
| C(113) | 4351(9) | 4234(5) | −1436(7) | 32(4) |
| C(114) | 5541(8) | 3686(6) | −1781(7) | 29(4) |
| C(115) | 5804(7) | 2642(6) | −1474(7) | 25(4) |
| C(116) | 4877(8) | 2147(5) | −822(7) | 24(3) |
| C(121) | 2309(8) | 877(5) | 82(6) | 16(3) |
| C(122) | 1770(9) | 159(6) | 802(5) | 22(3) |
| C(123) | 1459(9) | −741(6) | 525(7) | 30(4) |
| C(124) | 1687(9) | −924(5) | −471(8) | 32(4) |
| C(125) | 2226(9) | −207(7) | −1190(6) | 30(4) |
| C(126) | 2537(9) | 694(6) | −914(6) | 26(4) |
| C(131) | 876(6) | 2833(6) | 262(6) | 16(3) |
| C(132) | 405(8) | 2981(6) | −701(5) | 20(3) |
| C(133) | −874(8) | 3508(6) | −877(5) | 24(3) |
| C(134) | −1682(6) | 3887(6) | −90(6) | 19(3) |
| C(135) | −1211(7) | 3739(7) | 874(6) | 23(3) |
| C(136) | 67(8) | 3212(6) | 1050(5) | 19(3) |

[a] $U_{eq}$ is defined as one third of the trace of the orthogonalized $U_{ij}$ tensor.

Table 5
Atomic coordinates ($\times 10^4$) and equivalent isotropic displacement parameters ($Å^2 \times 10^3$) for [($\mu$-H)$Os_3(CO)_9$\{$\mu$-1,2-$\eta^2$-$C_9H_5(CH_3)N$\}-\{$P(OMe)_3$\}] **14**

| | $x$ | $y$ | $z$ | $U_{eq}^a$ |
|---|---|---|---|---|
| Os(1) | 2119.2(3) | 1099.2(2) | 2056.8(4) | 14(1) |
| Os(2) | 1373.3(3) | −549.6(2) | 1810.3(4) | 14(1) |
| Os(3) | 3411.0(3) | −221.1(2) | 2029.3(4) | 14(1) |
| P(1) | 3952(2) | −1490(2) | 1841(2) | 18(1) |
| O(1) | 646(7) | 2383(4) | 2217(7) | 38(2) |
| O(2) | 3970(7) | 1944(5) | 3413(6) | 39(2) |
| O(3) | 2473(6) | 1791(4) | −202(6) | 30(2) |
| O(4) | 5400(6) | 589(5) | 2385(7) | 39(2) |
| O(5) | 2922(6) | 1(4) | −591(6) | 31(2) |
| O(6) | 3684(6) | −460(4) | 4638(7) | 27(2) |
| O(7) | −830(7) | −761(5) | 1348(7) | 31(2) |
| O(8) | 1951(6) | −2241(4) | 2726(7) | 35(2) |
| O(9) | 1201(6) | −1120(5) | −636(6) | 33(2) |
| O(10) | 3144(6) | −2029(4) | 1045(6) | 24(2) |
| O(11) | 4295(5) | −2027(4) | 2960(6) | 23(2) |
| O(12) | 4893(6) | −1592(4) | 1376(7) | 30(2) |
| N(1) | 1504(6) | −78(5) | 3505(7) | 16(2) |
| C(1) | 1180(9) | 1899(7) | 2135(9) | 24(3) |
| C(2) | 3247(9) | 1616(6) | 2906(9) | 22(3) |
| C(3) | 2308(9) | 1497(6) | 578(10) | 23(3) |
| C(4) | 4656(10) | 277(6) | 2261(9) | 25(3) |
| C(5) | 3089(8) | −79(6) | 404(9) | 14(2) |
| C(6) | 3557(8) | −353(6) | 3658(11) | 17(3) |
| C(7) | 6(10) | −650(6) | 1558(9) | 19(3) |
| C(8) | 1732(9) | −1595(7) | 2349(10) | 28(3) |
| C(9) | 1280(8) | −883(6) | 282(10) | 22(3) |
| C(10) | 3306(9) | −2882(6) | 833(11) | 40(4) |
| C(11) | 5192(10) | −1853(7) | 3759(11) | 51(4) |
| C(12) | 4949(10) | −1230(7) | 306(11) | 40(4) |
| C(13) | 1895(8) | 640(6) | 3599(9) | 16(3) |
| C(14) | 2136(9) | 1051(7) | 4690(9) | 24(3) |
| C(15) | 2022(8) | 715(6) | 5656(10) | 23(3) |
| C(16) | 1529(8) | −44(6) | 5544(9) | 17(3) |
| C(17) | 1305(8) | −448(6) | 6505(10) | 24(3) |
| C(18) | 823(8) | −1152(6) | 6342(10) | 22(3) |
| C(19) | 543(9) | −1493(6) | 5302(10) | 29(3) |
| C(20) | 754(8) | −1159(6) | 4330(9) | 18(3) |
| C(21) | 1264(8) | −426(6) | 4449(9) | 17(3) |
| C(22) | 2323(9) | 1125(7) | 6836(9) | 32(3) |

[a] $U_{eq}$ is defined as one third of the trace of the orthogonalized $U_{ij}$ tensor.

## Acknowledgements

This work was supported by the Fonds der Chemischen Industrie and by the Commission for the European Communities. SEK gratefully acknowledges the Alexander von Humboldt Foundation for a fellowship and Royal Society of Chemistry for partial support. MBH and KMAM acknowledge the EPSRC for support of the X-ray facilities at Cardiff.

## References

[1] M. Day, D. Espitia, K.I. Hardcastle, S.E. Kabir, E. Rosenberg, R. Gobetto, L. Milone, D. Osella, Organometallics 10 (1991) 3550.
[2] S.E. Kabir, E. Rosenberg, M. Day, K.I. Hardcastle, M. Irving, J. Cluster Sci. 5 (1994) 481.
[3] M. Day, D. Espitia, K.I. Hardcastle, S.E. Kabir, T. McPhillips, E. Rosenberg, R. Gobetto, L. Milone, D. Osella, Organometallics 12 (1993) 2309.
[4] A. Rellinghalli, A. Tiripicchio, J.A. Cabeza, S.A. Oro, J. Chem. Soc. Dalton Trans. (1990) 1509.
[5] K.A. Azam, R. Dilshad, S.E. Kabir, K. Khatoon, L. Nessa, M.M. Rahman, E. Rosenberg, M.B. Hursthouse, K.M.A. Malik, A.J. Deeming, J. Chem. Soc. Dalton Trans. (1996) 1731.
[6] M.R. Churchill, B.G. DeBoer, F.J. Rotella, Inorg. Chem. 15 (1976) 1843.
[7] M.R. Churchill, B.G. DeBoer, F.J. Rotella, Inorg. Chem. 15 (1976) 878.
[8] R.J. Gillespie, I. Hargittai, The VSEPR Model of Molecular Geometry, Allyn & Bacon, Boston, 1991, p. 19.
[9] (a) A.J. Deeming, S. Donovan-Mtunzi, S.E. Kabir, M.B. Hursthouse, K.M.A. Malik, N.P.C. Walker, J. Chem. Soc. Dalton Trans. (1987) 1869. (b) A.J. Deeming, K.I. Hardcastle, S.E. Kabir, J. Chem. Soc., Dalton Trans. (1988) 827. (c) W.G. Feighery, R.D. Allendoerfer, J.B. Keister, Organometallics 9 (1990) 2424.
[10] M.I. Bruce, M.J. Liddell, C.A. Hughes, J.M. Patrick, B.W. Skelton, A.H. White, J. Organomet. Chem. 347 (1988) 181.
[11] B.F.G. Johnson, J. Lewis, E. Nordlander, P.R. Raithby. J. Chem. Soc. Dalton Trans. (1996) 755.
[12] (a) S.B. Colbran, P.T. Irele, B.F.G. Johnson, F.J. Lahoz, J. Lewis P.R. Raithby, J. Chem. Soc., Dalton Trans. (1989) 2023. (b) C. Jangala, E. Rosenberg, D. Shinner, S. Aime, L. Milone, E. Sappa, Inorg. Chem. 19 (1980) 1571. (c) E.J. Ditzel, B.F.G. Johnson, J. Lewis, J. Chem. Soc. Dalton Trans. (1987) 1289.
[13] (a) S.E. Kabir, D.S. Kolware, E. Rosenberg, K.I. Hardcastle, W. Creasswell, J. Grindstaff, Organometallics 14 (1995) 3613. (b) A. Eisenstadt, C.M. Giandomenico, M.F. Frederick, R.M. Laine, Organometallics 4 (1985) 2033.
[14] J.A. Darr, S.R. Drake, M.B. Hursthouse, K.M.A. Malik, Inorg. Chem. 32 (1993) 5704.
[15] N.P.C. Walker, D. Stuart, Acta Crystallogr. Sect. A 39 (1983) 158; adapted for FAST geometry by A.I. Karaulov, University of Wales, 1991.
[16] G.M. Sheldrick, Acta Crystallogr. Sect. A 46 (1990) 467.
[17] G.M. Sheldrick, SHELXL93 program for crystal structure refinement, University of Göttingen, 1993.
[18] K. Davies, SNOOPI program for crystal structure drawing, University of Oxford, 1983.